R-08-80

System and safety studies of accelerator driven systems for transmutation

Annual report 2007

Vasily Arzhanov, Andrei Fokau, Calle Persson,
Odd Runevall, Nils Sandberg, Milan Tesinsky,
Janne Wallenius, Youpeng Zhang

Division of Reactor Physics
Royal Institute of Technology

May 2008

Svensk Kärnbränslehantering AB
Swedish Nuclear Fuel
and Waste Management Co
Box 250, SE-101 24 Stockholm
Tel +46 8 459 84 00

ISSN 1402-3091
SKB Rapport R-08-80

System and safety studies of accelerator driven systems for transmutation

Annual report 2007

Vasily Arzhanov, Andrei Fokau, Calle Persson,
Odd Runevall, Nils Sandberg, Milan Tesinsky,
Janne Wallenius and Youpeng Zhang.

Division of Reactor Physics
Royal Institute of Technology

May 2008

Summary

Within the project “System and safety studies of accelerator driven systems for transmutation”, research on design and safety of sub-critical reactors for recycling of minor actinides is performed. During 2007, the reactor physics division at KTH has calculated safety parameters for EFIT-400 with cermet fuel, permitting to start the transient safety analysis. The accuracy of different reactivity meters applied to the YALINA facility was assessed and neutron detection studies were performed. A model to address deviations from point kinetic behaviour was developed. Studies of basic radiation damage physics included calculations of vacancy formation and activation enthalpies in bcc niobium. In order to predict the oxygen potential of inert matrix fuels, a thermo-chemical model for mixed actinide oxides was implemented in a phase equilibrium code.

The Lic. Eng. thesis “Reactivity Assessment in Subcritical Systems” was presented by Calle Persson in May 2007.

Sammanfattning

I projektet ”System- och säkerhetsstudier av acceleratordrivna system för transmutation” utförs forskning om design och säkerhet för underkritiska reaktorer avsedda att förbränna andra aktinider än uran och plutonium. Under 2007 har avdelningen för reaktorfysik på KTH beräknat säkerhetsparametrar för EFIT-400 med cermet-bränsle, som kommer att användas i transientanalys. Precisionen i olika metoder för att mäta reaktivitet har provats vid experiment med YALINA, där även neutrondetektionsteknik har studerats. En teoretisk modell för att ta hänsyn till avvikelser från punktkinetiskt beteende har utvecklats. Studier av grundläggande strålskadefysik har innefattat beräkningar av vakansformations- och aktiveringsenergier i niob med bcc-struktur. Beräkningar av syrepotential i inerta matrisbränslen har förberetts genom att implementera en termokemisk model för blandade aktinidoxider i en fasjämviktskod.

Licentiatavhandlingen ”Reactivity Assessment in Subcritical Systems” försvarades av Calle Persson i Maj 2007.

Contents

1	**Introduction**	7
2	**Safety studies of XT-ADS and EFIT**	9
2.1	Neutronic analysis	9
2.2	Transient analysis	10
3	**Sub-criticality monitoring**	11
3.1	The YALINA experiments	11
3.2	YALINA-Thermal	11
3.3	YALINA-Booster	11
3.4	General Conclusions	11
3.5	Future Applications	12
3.6	Neutron detection at YALINA	13
3.7	Deviations from point kinetics	14
4	**Fuel modelling**	17
4.1	Introduction	17
4.2	The oxygen potential of actinide dioxides	17
5	**Modelling of radiation damage**	19
6	**References**	21
7	**List of publications**	23
8	**List of participation in conferences and project meetings**	25

1 Introduction

Research on accelerator driven systems (ADS) for transmutation of nuclear waste is performed at the division of reactor physics at KTH. Presently, the major context of this research is the EUROTRANS project in the 6th framework programme of the European Commission, where design of an experimental ADS with MOX fuel and lead-bismuth coolant (XT-ADS) and an industrial demonstration facility for minor actinide transmutation (EFIT) is made. Development of ADS fuel and structural materials are integrated into the project.

The division of reactor physics at KTH is participating in all domains of the EUROTRANS project, in particular with the following activities:

Domain DESIGN:	Co-ordination of the safety work package. Assessment of the source term in case of severe accidents.
Domain ECATS:	Development and testing of methods for sub-criticality monitoring.
Domain AFTRA:	Fuel modelling, Transient safety analysis.
Domain DEMETRA:	Modelling of radiation damage in Fe-Cr-C steels.

Furthermore, KTH coordinated the 6th FP RedImpact project. In this project, scenario studies of partitioning and transmutation and their impact on geological repository design and performance is assessed.

In the present report, a summary of activities performed during 2007 is provided, including an account for participation in conferences and project meetings.

2 Safety studies of XT-ADS and EFIT

2.1 Neutronic analysis

During 2007, the main research activity was an analysis of the EFIT-400 accelerator driven system with Mo-matrix fuel at BOC. On the basis of specification provided by FZK and SCK, a model of the system was created for Monte Carlo simulation with MCNP 4c3 and MCNPX 2.5. A number of simulations have been done for determination and analysis of multiplication properties of the reactor, as well as flux and power distributions. Basic safety parameters of the system have been evaluated for the reactor safety analysis. The results have been compared with ones calculated by FZK with a deterministic code and good agreement has been achieved. By analyzing an impact of different nuclear data libraries, significant discrepancy between JEFF3.0 and JEFF3.1 libraries was found.

EFIT-400 with Cermet fuel (molybdenum matrix) is loaded with 216 fuel assemblies with total mass of 7.5 ton actinide fuel. The fuel consists of 46% of Pu and 54% of Np, Am and Cm. The fuel assemblies are arranged in three fuel zones. The core is cooled by pure lead. The source of initial neutrons is a proton accelerator beam of 800 MeV which hits a lead spallation target in the center of the core.

Table 2-1. Neutronic parameters for EFIT-400 obtained with MCNP and MCNPX.

	MCNP		SIMMER by FZK		
	JEFF 3.1	JEFF 3.0	JEFF 3.1	ENDFB7	SIMMER
Keff	0.98317 ± 0.00019	0.93955 ± 0.00019	0.98204	0.96473	0.97336
Void worth, pcm	4,850 ± 28	N/A	6,403	5,978	7,355

	Keff	Reactivity, $	Beff, pcm	Void worth, pcm
KTH, JEFF 3.1	0.98317 ± 0.00019	–9. 8 ± 1.7	175 ± 31	4850 ± 28 (27.7 ± 4.9 $)
FZK, SIMMER	0.97336	–14.18	192	7,355

Keff	Source mult, n/p	Ksrc	Source efficiency
0.98317 ± 0.00019	20.3 ± 0.1	0.96295 ± 0.00013	0.445 ± 0.005

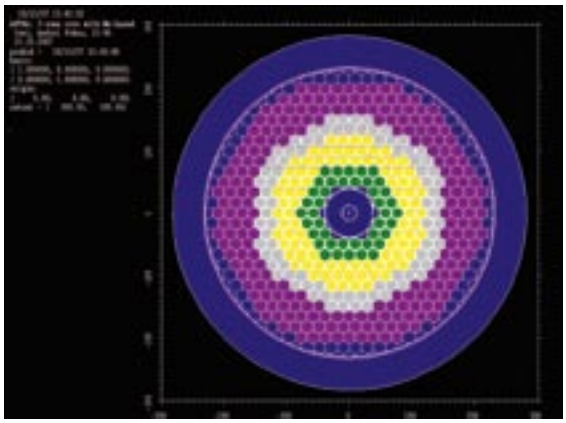

Figure 2-1. *Core Map of EFIT-400 with Cermet fuel.*

2.2 Transient analysis

The thermophysical properties of oxide and nitride fuels were reviewed for application in transient analysis using the SAS4A code. Preliminary results for EFIT-400 were obtained for unprotected loss of flow (ULOF), unprotected transient over power (UTOP) and unprotected loss of heat sink (ULOHS). These results will be revised as the core design for EFIT becomes frozen in 2008.

3 Sub-criticality monitoring

3.1 The YALINA experiments

Through the YALINA-experiments, reactivity determination methods have been investigated experimentally in the region $0.90 < k_{eff} < 0.98$. In the following, some specific conclusions from YALINA-Thermal and YALINA-Booster are presented followed by some general conclusions and future applications of the results.

3.2 YALINA-Thermal

Through the YALINA-Thermal experiments, it was found that the PNS slope fitting method is less reliable when there is no fundamental mode. However, in this study, the prompt neutron decay constant could be estimated through multiple exponential fitting since a fundamental mode was visible in the reflector channels. Hence the PNS slope fitting method is preferable closer to criticality. In complete absence of a fundamental mode, a theoretical model describing the neutron flux after a neutron pulse insertion must be applied. Based on this model, the kinetic parameters can be adjusted to find the best fit to the measured neutron flux.

It was shown that the area method gives a value of the reactivity with a certain spatial spread. However, this value deviated slightly from the value obtained through simulations. Compared to MCNP, the effective multiplication factor was underestimated by the area method. However, the area method delivers a result with high statistical accuracy.

In this study, the source jerk method was just demonstrated. Although it did not reproduce the result of the other methods for one source interruption it has probably a potential for reactivity monitoring if used in repeated mode.

3.3 YALINA-Booster

In the YALINA-Booster experiments it was found that the PNS slope fitting technique is very stable closer to criticality. The area method still suffer from spatial dependence also around $k_{eff} = 0.97$ as it did around $k_{eff} = 0.90$ in YALINA-Thermal. However, with the area method it is possible to measure reactivity differences with low spatial spread.

In these experiments, the continuous source Rossi-α and Feynman-α methods were not reliable in their classical definitions for low keff. The agreement with the PNS measurements was better for the less subcritical configuration.

The pulsed Rossi-α is reliable but unnecessarily complicated, since the result can be achieved directly through slope fitting of the PNS histogram.

3.4 General Conclusions

By reconsidering the list of requirements of an online reactivity meter one can find that actually none of the studied method fulfills all the criteria (short measurement time, low spatial dependence, high accuracy, detector type and neutron source independence). The requirement of short measurement time was fulfilled only by the source jerk method, but this method suffers from low accuracy. The PNS slope fitting method has low spatial dependence, but is more difficult to apply if there is no fundamental mode. On the other hand, the area method delivers results

with high accuracy but with a certain spatial dependence. Further, the measurement time is long for both methods. Long measurement times are experienced also when applying the noise methods and the results from those methods are generally not trustworthy for deep subcriticalities. Moreover, the noise methods will probably not work for higher power levels, when passing the neutron noise threshold. The last two features, detector type and neutron source independence, were not investigated in this study.

3.5 Future Applications

The work made has provided deeper understanding in the most frequently used methods for subcriticality measurements, but apparently there is more work to be performed in order to find a suitable reactivity meter for subcritical systems. Concerning ADS, there are essentially two regions of applications for reactivity determination methods: fuel loading and regular operation. During loading of the core, most probably the inverse multiplication method will be used, as when loading any core. However, this method does only tell the operator when the core will become critical and does not tell how subcritical the core is. At some point k_{eff} must be known in order to find a suitable operation configuration. In this case, some of the methods used in this study may be used; the area method, which seems to be reliable in the region for ADS operations, is probably a good choice. A problem is, however, that β_{eff} must be known in order to translate the result of the measurement, given in dollars, to k_{eff}. For uranium and plutonium based systems this parameter can easily be calculated. Moreover, it has been measured for several systems historically. However, for cores loaded with high fractions of americium and curium, this is not as straight forward. The quality of the delayed neutron data for these isotopes is not as good as for uranium and plutonium, and measurements of β_{eff} for such systems have probably never been performed.

For the regular operation of an ADS, the current-to-flux measurement technique has been proposed By measuring the proton beam current, I_p, and the neutron flux somewhere in the core a reactivity dependent ratio, R, is obtained:

$$R(\rho) = c\frac{I_p}{\varphi}, \quad \rho < 0$$

Any change in R without a preceding change in beam current, may be interpreted as resulting from a reactivity change. The factor c may be calibrated with the traditional reactivity determination methods and it is here assumed that the neutron source strength is directly proportional to the beam current. The current-to-flux method seems to be a reliable tool for online monitoring, but it has not yet been verified.

Another related method, which probably can be performed in parallell with the current-to-flux measurement, is the repeated source jerk experiment. The source operates with short interruptions of length t_I with frequency $f = 1/T$ according to Figure 3-1. After the source interruption the beam starts again and operates during the time t_B, obeying:

$$T = t_I + t_B$$

The expected corresponding neutron flux is depicted in Figure 3-2. Starting from neutron flux level n_0, the neutron flux will decay following the prompt neutron decay constant, α, to a semi-stable flux level n_1. The level n_1 will decrease slowly following the decay of the delayed neutron precursors. The neutron flux level n_B indicates the inherent source of spontaneous fissions etc. After several beam interruptions the level n_1 can be estimated with high accuracy and the reactivity in dollars can be calculated as:

$$\frac{\rho}{\beta_{eff}} = \frac{(n_1 - n_B) - (n_0 - n_B)}{(n_1 - n_B)} = \frac{n_1 - n_0}{n_1 - n_B}$$

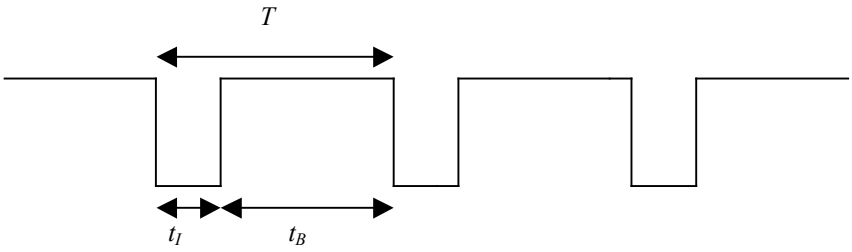

Figure 3-1. *Neutron source characteristics for the repeated source jerk experiment.*

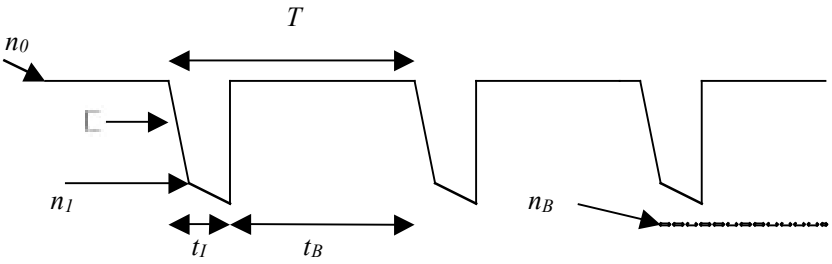

Figure 3-2. *Expected neutron flux characteristics following the source variations in Figure 3-1.*

In addition, through this experiment the prompt neutron decay constant, α, can be found. When using this method in a full power ADS, t_I must be in the scale of a millisecond, not to induce thermal variations accompanied by induction of stress in the construction materials. Also this method has not yet been evaluated experimentally.

Although the methods studied in this thesis do not fulfil the requirements for being candidates for online reactivity monitoring, they will serve as tools for calibration of the possible future techniques presented here; in particular the combined PNS slope fitting and area methods.

3.6 Neutron detection at YALINA

Monte Carlo simulations of the core were made with MCNP. to assess periphery flux measurements by ^{3}He counters. The experimental results were compared with the simulation and by means of making small changes in the simulations, the shape of the periphery flux was explained (Figure 3-3).

The calculations were performed for two different configurations. Besides the periphery flux investigation, other MCNP calculations were done to confirm experimental results of reaction rates measurements. The measurements were done by irradiating a set of activation foils and the results of the MCNP calculation are compared by means of reaction rates for different activation reactions. In this part, the full agreement was not yet achieved and searching for the real reason is still in progress. The last group of the YALINA-Booster calculations resulted in description of radial distribution of the thermal and epithermal neutron flux. This experiment was also done for real and studies the changes of the neutron flux across the core.

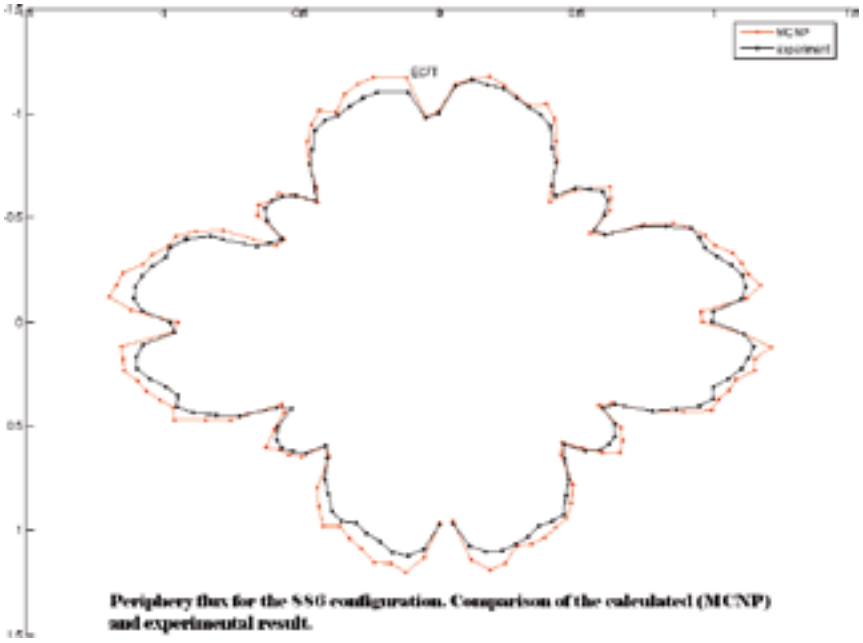

Figure 3-3.

3.7 Deviations from point kinetics

In order to estimate the reactivity of the YALINA experiment, one typically applies techniques such as Feynmann-alpha or N.G. Sjöstrand methods, that are essentially based on the assumption of the point kinetic behaviour of the system in question. Normally these methods work very well, however a number of peculiarities was observed in the YALINA experiment that are difficult to explain within the framework of the point kinetic model. One of such examples is presented in Figure 3-4.

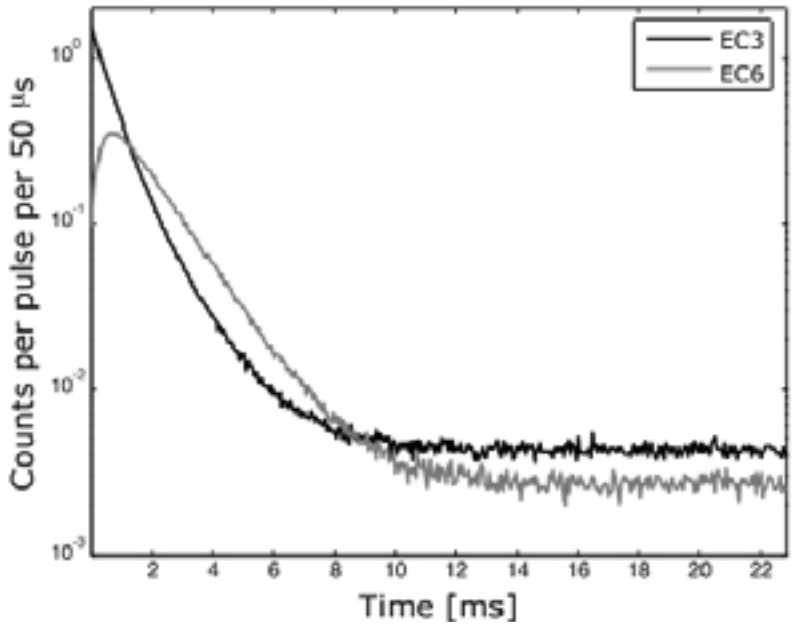

Figure 3-4. *Experimental data from two different detectors.*

As seen in the picture, one of the signals has a peak whereas the other does not. In an attempt to explain this peculiarity, a simple diffusion model with delayed neutrons was considered. More specifically, it was assumed one prompt and one average delayed neutron group in the infinite slab geometry.

$$\begin{cases} \dfrac{1}{v}\dfrac{\partial \Phi(x,t)}{\partial t} = D\dfrac{\partial^2 \Phi(x,t)}{\partial x^2} + \left[(1-\beta)\nu\Sigma_f - \Sigma_a\right]\Phi(x,t) + \lambda C(x,t) \\ \dfrac{\partial C(x,t)}{\partial t} = \beta\nu\Sigma_f \Phi(x,t) - \lambda C(x,t) \end{cases}$$
$$-\infty < x < \infty, \quad 0 \le t < \infty$$

The solution to this equation was found to be:

$$\phi(z,\tau) = \frac{1}{2l\sqrt{\pi\tau}} e^{-\tau - \frac{z^2}{4\tau}} - \frac{2\xi}{\sqrt{\pi}\gamma^2}\sqrt{\tau}\, e^{-\tau - \frac{z^2}{4\tau}} + \frac{\xi}{2\gamma^3} e^{-\lambda n \tau} \times$$
$$\times \left[e^{-\gamma z}(\gamma z + 1)\operatorname{erfc}\left(\frac{z}{2\sqrt{\tau}} - \gamma\sqrt{\tau}\right) + e^{\gamma z}(\gamma z - 1)\operatorname{erfc}\left(\frac{z}{2\sqrt{\tau}} + \gamma\sqrt{\tau}\right)\right]$$

Here, z and τ are scaled space and time variables. This solution represents a neutron distribution following a neutron pulse at the origin at time zero.

It can be shown that the solution close to the origin has a non-peaked shape. What is more important the solution represents peaked signals too as seen in Figure 3-5. It gives grounds to believe that the derived analytical solution may turn out to be able to to explain and extract the reactivity and other important parameters from detector signals.

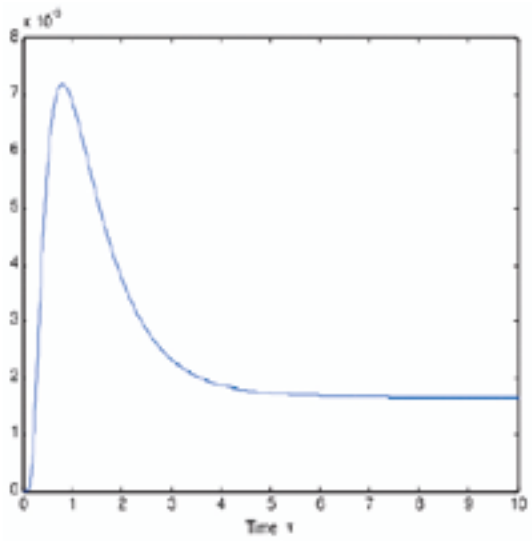

Figure 3-5. *Time behaviour of the solution far from the origin.*

4 Fuel modelling

4.1 Introduction

The main focus during 2007 has been to develop thermochemical models for oxide based transmutation fuels under irradiation. Firstly, a model of the actinide dioxide phase has been established. This work is presented below. Secondly work has begun on a thermodynamic database and models for the different fission product phases which can be expected to exist in the fuel. All this is done in collaboration with NRG in Petten and ITU in Karlsruhe.

To also understand the gas transport phenomena in the fuel matrix, helium diffusion in molybdenum was studied using ab initio methods. This work is still under progress and results are expected during 2008.

4.2 The oxygen potential of actinide dioxides

The oxygen potential is a key property of oxide-based nuclear fuels. It has a major impact on clad oxidation and, in the case of composite fuels, oxidation of fuel components. It also influences the chemical form of fission products in the fuel. Therefore, oxygen potential models of in-pile conditions are of interest. As future reactor fuels can be expected to contain significant amounts of minor actinides and plutonium, the demand increases for more flexible oxygen potential models, both concerning composition and temperature. Therefore, the Lindemer-Besmann model /1/ was chosen to model the fluorite phase of the transmutation fuels, since it has proven to give good results for uranium, plutonium and americium dioxides separately. This model was developed using single variable calculus where all but one parameter was excluded using the mass balance equations. However, this is not possible in the case of mixed oxides where the mass balance equations are fewer than the number of compounds included in the model. The existing models for the uranium /1/, plutonium /2/ and americium dioxide /3/ were therefore implemented in a modern phase equilibrium calculation code. Since also the neptunium dioxide shows a tendency towards hypostoichiometry a model for this system was developed and implemented as well. The implemented data can be found in Table 4-1.

These models are based on the assumption that a non-stoichiometric compound consists of a solid solution of two compounds, one real and representing the stoichiometric regime, e.g. UO_2, one hypothetical representing the deviation from stoichiometry. The Gibbs energy of the hypothetical compound and, if needed, interaction parameters are determined from experimental data.

By assuming an ideal substitutional solution model in between different actinide compounds the oxygen potential of different mixed dioxides were predicted and compared with experimental data. Some examples are shown in Figure 4-1 and Figure 4-2.

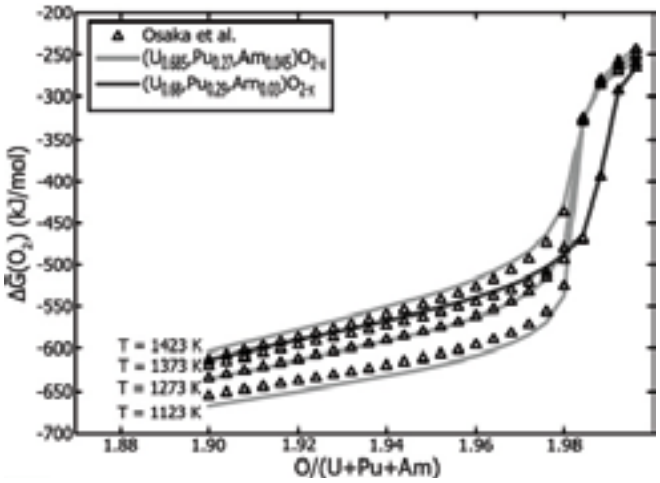

Figure 4-1. *The oxygen potential of (U, Pu, Am) $O_2 \pm x$, experimental points /6, 7/ and the model predictions.*

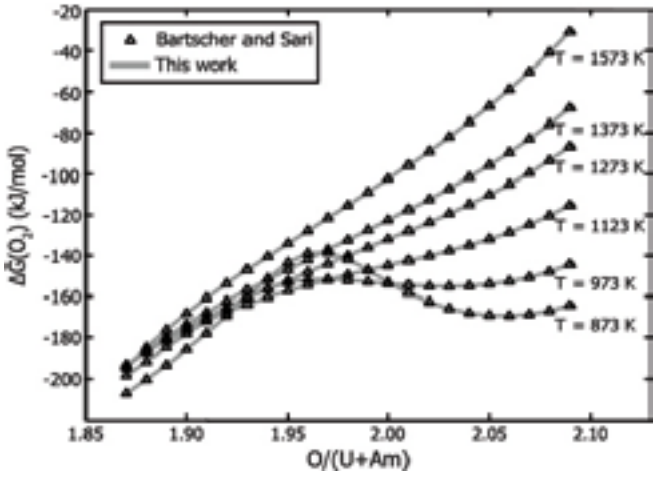

Figure 4-2. *The oxygen potential of (U, Am) $O_2 \pm x$, experimental points /8/ and model predictions.*

Table 4-1. The Thermodynamic data used in the presented assessment.

Compound	**Δ_f G**	**Ref.**
ThO_2	−1219192 + 177.42T	/4/
$U_{1/3}$	72422 − 18.4T	/1/
UO_2	−1080000 + 196.0T	/1/
$U_2O_{4.5}$	−2250000 + 391.4T	/1/
U_3O_7	−3396400 + 569.9T	/1/
NpO_2	−1068900 + 171.19T	/5/
$Np_{5/2}O_{9/2}$	−2374000 + 365.6T	This work
$Pu_{4/3}O_2$	−1091900 + 169.7T	/2/
PuO_2	−1047800 + 187.71T	/2/
$Am_{5/4}O_2$	−1107507 + 198.81T	/3/
AmO_2	−924068 + 167.47T	/3/
Interacting compounds	**Interaction term**	**Ref.**
$Pu_{4/3}O_2$, PuO_2	$x_{Pu4/3O2}x_{PuO2}(x_{Pu4/3O2}-x_{PuO2})(-41510+30.2T)$	/2/
$Am_{5/4}O_2$, AmO_2	$x_{Am5/4O2}x_{AmO2}(87573-59.25T)$	/3/

5 Modelling of radiation damage

In general, body centered cubic (bcc) materials are much more irradiation resistant compared to face centered cubic (fcc) materials. Thus, ferritic-martensitic (F–M) steels are superior to austenitic steels in this respect. In particular, some Fe-Cr based F–M steels show a much better resistantce to swelling compared to austenitic steels. The fundamental reason for this is however not completely understood. Some rather advanced models exist to explain this in terms of interstitial mobility, interstitial clustering and binding to solutes.

A predictive model of swelling in a specific alloy should be applicable to other types of alloys as well. An interesting system in this respect is V-5Fe. It has a bcc structure, but in contrast to Fe-Cr alloys it is known to resist irradiation very poorly. In fact, this system has the world record in swelling; 160% at 50 displacements per atom (dpa) /9/. It is obvious, therefore, that not only the crystal structure determines a materials responce to irradiation, but also other factors such as the defect-defect and defect-solute interactions.

In the current work, we have used first-principles electronic structure methods in order to study point-defect properties in Nb. The idea is to use Nb as a bench-mark system for first-principles calculations of defect properties in a bcc metal. Nb then has the benefit of being non-magnetic, which removes some complications when experimental data are interpreted. There are also a fairly large amount of data on vacancy-impurity interactions and impurity diffusion rates in Nb, which are in principle also attainable to first-principles calculations. We have focused on applying electronic structure methods in order to calculate i) the vacancy concentration and ii) the self-diffusion rate in pure Nb. The latter can be directly compared with experimental data. This comparison gives information on what accuracy that can be expected from similar calculations targeting defect-solute interactions, e.g. in V or Fe based alloys. Such numbers, in turn, are needed in quantitative and predictive models of swelling in bcc alloys.

Table 5-1 shows vacancy formation and migration parameters calculated by two different methods. First, electronic structure calculations based on density functional theory (DFT) were carried out, using the simulation package VASP. Second, an empirical model potential was used. In the DFT calculations, H_v was calculated using simulation cells of different size (54 and 128 atoms) and the convergence with respect to various numerical approximations was carefully tested. H_m was obtained in a similar calculation, and we also tested and ruled out other migration mechanisms (e.g. second nearest neighbour jumps).

The only parameter that we were unable to calculate is the prefactor for migration jumps. A possible explanation is the use of a 54 atom cell in this calculation. The transition state leads to more strain in the simulation cell compared to the formation of a vacancy, and it may be more appropriate to use a larger simulation cell. However, this leads to much more demanding calculations. A second factor is that Nb is known to have long-range force-interactions in a Born-von-Karman fit to measured phonon dispersion data. Phonon-dispersion curves and densities of states (DOS) are a by-product in our phonon calculations, and are compared with

Table 5-1. Calculated and experimental self-diffusion parameters. $H_D = H_v + H_m$ and $S_D = S_v + S_m$.

	VASP	Model potential	Experiments
H_v (eV)	2.85	2.50	2.6 ± 0.3
S_v (kB)	3.10	2.75	
H_D (eV)	3.77	3.31	4.1
S_D (kB)		5.0	5.2

measured ones in Figure 5-1. It is seen that a 128 atom cell is required to reproduce the main features of the experimental DOS, although a spurious peak at 4 THz is still present. Again, this indicates that it would be preferable to use a larger simulation cell in diffusion calculations on Nb. The calculated vacancy formation and migration parameters, with S_m taken from model potential calculations, can be put together to obtain the predicted self diffusion rate. It is shown in Figure 5-2, along with available experimental tracer diffusion data. The agreement between theory and experiments, both in terms of the self-diffusion activation enthalpy (given by the slope in Figure 5-2) and in terms of absolute self-diffusion rates, is surprisingly good, considering that the present calculations are to a large degree free of experimental input.

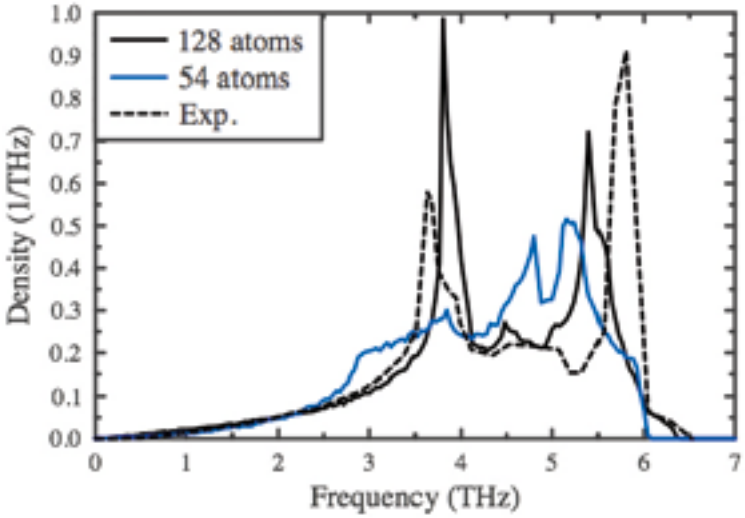

Figure 5-1. *Calculated phonon density of states. Experimental data from /10/.*

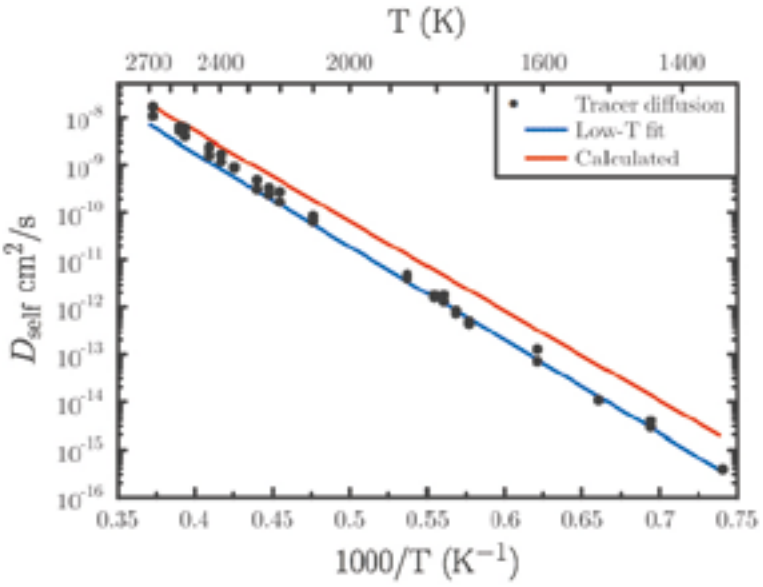

Figure 5-2. *Calculated and experimental self-diffusion rates in Nb.*

6 References

/1/ **Lindemer T B, Besmann T M, 1985.** J. Nucl. Mater. 130 (1985) 473–488.

/2/ **Besmann T M, Lindemer T B, 1985.** J. Nucl. Mater. 130 (1985) 489–504.

/3/ **Thiriet C, Konings R J M, 2003.** J. Nucl. Mater. 320 (2003) 292–298.

/4/ **Bakker K, Cordfunke E H P, Konings R J M, Schram R P C, 1997.** J. Nucl. Mater. 250 (1997) 1–12.

/5/ **Konings R J M, Morss L R, Fuger J, 2006.** In: The Chemistry of the Actinide and Transactinide Elements, Vol. 4, ed: L. R. Morss, N. M. Edelstein, J. Fuger, Springer Verlag, 2006, Ch. 19.

/6/ **Osaka M, Satoa I, Namekawa T, Kurosakib K, Yamanaka S, 2005.** J. Alloy. Compd. 397 (2005) 110–114.

/7/ **Osaka M, Kurosaki K, Yamanaka S, 2007.** J. Alloy. Compd. 428 (2007) 355–361.

/8/ **Bartscher W, Sari C, 1986.** J. Nucl. Mater. 140 (1986) 91–93.

/9/ **Fukumoto K, Kimura A, Matsui H, 1998.** J. of Nuclear Materials 258–263, 1431 (1998).

/10/ **Guthoff F, Hennion B, Herzig C, Petry W, Schober H R, Trampenau J, 1994.** J. Phys. Condensed Matter 6, 6211 (1994).

7 List of publications

Olsson P, Domain C, Wallenius J, 2007. Ab initio study of Cr interactions with point defects in bcc Fe. Physical Review B 75 014110 (2007).

Tucek K, Jolkkonen M, Janne Wallenius J, Gudowski W, 2007. Studies of an accelerator-driven transuranium burner with hafnium based inert matrix fuel. Nuclear Technology 157 (2007) 277.

Wallenius J, Olsson P, Malerba L, Terentyev D, 2007. Simulation of thermal ageing and radiation damage in Fe-Cr. Nuclear instruments and methods in physics research B 255 (2007) 68.

Talamo A, Gudowski W, 2007. Incineration of Light Water Reactors waste in High Temperature Gas Reactors: Axial Fuel Management and Strategy for Transmutation of Americium and Curium. Nuclear Science and Engineering 156 (2007) 244.

Talamo A, 2007. Analytical Calculation of the Average Dancoff Factor for Prismatic High Temperature Reactors. Nuclear Science and Engineering 156 (2007) 343.

Talamo A, 2007. Analytical Calculation of the Fuel Temperature Reactibity Coefficient for Pebble Bed and Prismatic High Temperature Reactors for Plutonium and Uranium-Thorium Fuels. Annals of Nuclear Energy, 34/1–2, pp. 68–82 (2007).

Westlen D, 2007. Reducing radiotoxicity in the long run. Progress in nuclear energy 49 (2007) 597.

Persson C-M, 2007. Reactivity Assessment in Subcritical Systems. Lic. Eng. Thesis, Division of Reactor Physics, KTH (2007).

Dufek J, 2007. Advanced Monte Carlo Methods in Reactor Physics, Eigenvalue and Steady State Problems. Lic. Eng. Thesis, Division of Reactor Physics, KTH (2007).

8 List of participation in conferences and project meetings

Andrei Fokau

- FJOH summer school in Karlsruhe, Germany, September 4–7.
- EUROTRANS AFTRA meeting. Petten, The Netherlands, October 24–25, 2007.

Calle Persson

- Young Generation annual meeting, Västerås, January 24–25 .
- EUROTRANS/ECATS kick-off meetingi Aix-en-Provence, France, January 31–February 01.
- EUROTRANS/ECATS meeting, Minsk, Belorussia, March 5–6.
- ANS annual meeting, Boston, USA, June 25–29.
- MCNPX Workshop in Santa Fe, New Mexico, USA, September 17–21.

Odd Runevall

- EUROTRANS AFTRA-meeting, ITU Karlsruhe, Germany, 21–22 March.
- Conference on Material Science &Technology, Detroit, USA, September 15–20.
- ACTINET project meeting, Karlsruhe, Germany, October 24–26
- Preparatory meerting for FAIRFUELs proposal, Amsterdam, The Netherlands, November 21.

Nils Sandberg

- 12th Fe-Cr workshop in Paris, France, December 10.
- Conference on Material Science &Technology, Detroit, USA, September 15–20.

Milan Tesinsky

- FJOH summer school in Karlsruhe, Germany, September 4–7.
- EUROTRANS AFTRA meeting. Petten, The Netherlands, October 24–25, 2007.

Janne Wallenius

- ACSEPT preparatory meeting, Paris, France, January 16.
- Asia-link board meeting in Torino, Italy, January 29–30.
- ACSEPT preparatory meeting in Amsterdam, The Netherlands, February 28.
- PATEROS meeting in Saclay, France, March 27.
- EUROTRANS DESIGN meeting, Lisbon, Portugal, March 28–30.
- EUROTRANS Governing Council meeting, Aix-en-Provence, April 26–27.
- 11th Fe-Cr workshop in Karlsruhe, Germany, May 7–8.
- EUROTRANS WP 1.5 meeting, Stockholm, May 22–23.

- SMINS workshop in Karlsruhe, June 4–5.
- Red Impact meeting in Sigtuna, June 21–22.
- ELSY meeting in Brussels, Belgium, July 3.
- Asia-link board meeting in Beijing, China, July 16–17.
- PATEROS meeting in Karlsruhe, Germany, September 4–5.
- FJOH summer school in Karlsruhe, Germany, September 4–7.
- EUROTRANS DEMETRA meeting, Karlsruhe, September 18, 21.
- Red Impact final workshop, Jülich, Germany, September 19–20.
- MATGEN-IV summer school, Cargese, France, October 1–5.
- HTR project meeting, Delft, The Netherlands, October 17.
- AFRODITE preparatory meeting, Obninsk, Russia, October 31.
- EUROTRANS WP 1.5 meeting, Madrid, Spain, November 13–14.

Youpeng Zhang

- FJOH summer school in Karlsruhe, Germany, September 4–7.
- MATGEN-IV summer school, Cargese, France, October 15.
- EUROTRANS AFTRA meeting. Petten, The Netherlands, October 24–25, 2007.